CLASSIFYING MEADOW HYDROGEOMORPHIC TYPES WITH LIDAR AND MULTISPECTRAL IMAGERY USING OBIA

A Thesis submitted to the faculty of
San Francisco State University
In partial fulfillment of
the requirements for
the Degree

Master of Science

In

Geographic Information Science

by

Austen Anthony Lorenz

San Francisco, California

January 2017

CERTIFICATION OF APPROVAL

I certify that I have read Classifying Meadow Hydrogeomorphic Types with LiDAR and Multispectral Imagery Using OBIA by Austen Anthony Lorenz, and that in my opinion this work meets the criteria for approving a thesis submitted in partial fulfillment of the requirement for the degree Master of Science in Geographic Information Science at San Francisco State University.

Leonhard Blesius, Ph.D.
Associate Professor of Geography

Jerry Davis, Ph.D.
Professor of Geography

CLASSIFYING MEADOW HYDROGEOMORPHIC TYPES WITH LIDAR AND MULTISPECTRAL IMAGERY USING OBIA

Austen Anthony Lorenz
San Francisco, California
2017

Meadows play important ecological roles in the Sierra Nevada landscape. They slow flood waters, improve water quality, and provide valuable wildlife habitat. Knowing where and how many meadows exist is critical for researcher and land managers. This study demonstrated a remote sensing method using OBIA for semi-automated detection and classification of meadows. The study area was located within the Tahoe National Forest, USA. Using LiDAR and multispectral satellite imagery, meadows were detected and classified by hydrogeomorphic types. The hydrogeomorphic classes were defined with unique physical characteristics related to landform and water features. Meadows were detected using multispectral imagery and LiDAR derivatives. Detected meadows were then classified by hydrogeomorphic type using LiDAR derivatives. Accuracy assessments were conducted comparing the results to manually detected and classified meadows and an existing meadow database. The overall accuracy when compared to the manually detected meadows was 98% and to the hydrogeomorphic classification was 82%. The presented methods for meadow detection and hydrogeomorphic classification could be a valuable tool for land managers.

I certify that the Abstract is a correct representation of the content of this thesis.

Chair, Thesis Committee　　　　　　　　　　　　Date

ACKNOWLEDGEMENTS

There are several people I would like to acknowledge. First, I'd like to acknowledge Leonhard Blesius and Jerry Davis for their work on my thesis committee. A big thanks to the Tahoe National Forest for providing me with the data needed to complete this research. I'd like to thank the weekend map library crew for the inspiration and camaraderie. The AAG Boston group for making research fun. Jarrad Fisher for suggesting San Francisco State and for taking classes with me from third grade through graduate school. And my meadow fellow meadow researcher Darren Blackburn for working with me on group projects and researching meadows.

TABLE OF CONTENTS

LIST OF TABLES

LIST OF FIGURES

1 Introduction

Meadows occupy only a small fraction of the total land area in the Sierra Nevada, but play an important ecological role in the landscape[1]. They reduce the impact of floods by spreading the water out across their flat surface and slowing the water velocity, thereby delaying and reducing peak runoff [2,3]. Meadows improve the quality of water delivered to the surrounding watershed by filtering out sediment[3,4]. Large amounts of soil nitrogen and carbon are stored in meadows compared to other land cover types in the Sierra Nevada[5]. Finally, Sierra Nevada meadows provide critical habitat for endangered fish such as Lahontan cutthroat trout (*Oncorhynchus clarkii* henshawi), Eagle Lake rainbow trout (*Oncorhynchus mykiss* aquilarum), and California golden trout (*Oncorhynchus mykiss* aguabonita), and are important for many mammals, birds, amphibians, and reptiles[3,6–8].

Meadows in the Sierra Nevada are diverse; however, most feature shallow groundwater within one meter of the surface, herbaceous vegetation, and fine soils[9]. In the drier, warmer southern Sierra Nevada, meadows are found at higher elevations between 1,500 to 3,000 m elevation; in the wetter, cooler northern Sierra Nevada meadows are found at lower elevations between 300 to 2,700 m [10]. Meadows can range in size from a few square meters to several square kilometers[11].

Researchers have developed many classification schemes using a combination of biotic and abiotic features, such as soil moisture, vegetation, and elevation, to characterize meadows[1,4,10,12,13]. One such classification, initially developed to describe wetlands, is hydrogeomorphic classification, which characterizes meadows according to geomorphic and hydrologic features[14]. Hydrogeomorphology often determines the biotic systems and functions within meadows[9,14]. Hydrogeomorphic meadow classification can aid in the management of and communication about meadows, allowing researchers and resource managers to more accurately differentiate function and value according to meadow class [9].

Knowing how many and where meadows exist is critical for land managers; yet in the Sierra Nevada, there are still many undocumented meadows. Viers et al. (2013) estimated there to be 17,000 meadows over 0.4 ha in the Sierra Nevada. However, detecting and classifying meadows across an entire mountain range can be an arduous task.

Meadows have been detected and classified using a variety of methods. Known meadows have been mapped and classified in the field using GPS, in the office by hand tracing the outlines on aerial photographs and satellite images, or digitized from previous mapping efforts [15,16]. Unknown meadows have been detected and mapped manually by technicians systematically reviewing satellite imagery and air photos. Most of these methods are time intensive. Semi-automated and automated remote sensing can aid in efficiently detecting and classifying meadows, but few studies use this method for meadow detection and mapping [15,17]. Developing remote sensing methods for semi-automated and automated detection and classification of meadows would aid in their management.

While few remote sensing studies have been conducted on meadows, many studies have been conducted on wetlands throughout the world. Traditional pixel-based remote sensing methods for wetland detection have relied on the spectral values of individual pixels. Pixel-based methods work well with low to medium resolution imagery or data, such as Landsat TM with 30 meter resolution [18]. However, these methods do not work well with high resolution imagery or data imagery such as light detection and ranging (LiDAR). The use of high resolution imagery in a pixel-based analysis can cause misclassification due to small details such as shadows; this misclassification is known as salt and pepper [19]. Often, pixel-based analysis is inadequate for high resolution data[20].

Alternatively, Object-based image analysis (OBIA) is a technique that can improve the classification of high resolution imagery data. OBIA evaluates data by applying context and relationships to objects. OBIA starts by segmenting pixels into primitive objects based on algorithms that look at homogeneity and shape of the objects. OBIA maximizes similarities within objects and differences between objects [21]. This process requires testing different object size and shape parameter combinations to achieve a segmentation that best represents the phenomena being mapped [22]. Once the image has been segmented into primitive objects, the objects are classified. One such classification method is supervised decision tree classification, which creates hierarchical classes using a series of logical rules. Rules are based on object properties such as mean spectral reflectance within an object, segment shape (e.g., relationship between segment area and perimeter), or topological attribute (e.g., relationship to other segments) [21]. Objects may be further manipulated and refined until a classification accurately represents what is being mapped[20].

The aim of this study was to develop a remote sensing method using OBIA for semi-automated detection and classification of meadows. Specifically, the objectives of this study were (1) to detect meadows using LiDAR and multispectral imagery and (2) to classify detected meadows according to hydrogeomorphic type using physical characteristics derived from LiDAR.

2 Methods

2.1 Study Area

A 1000 km^2 area of the Tahoe National Forest (Fig. 1) was chosen for this study because it was representative of the complex landscape of the Sierra Nevada. The elevation ranges from 871 to 2,787m. Mean annual precipitation recorded from 1896 to 2012 at Bowman Dam, CA, in the western portion of the study area, was 1645.4 mm while the mean annual precipitation recorded at Sagehen Creek, CA east of the study site was 850 mm[23,24]. Most of the precipitation came in the winter months[23,24].

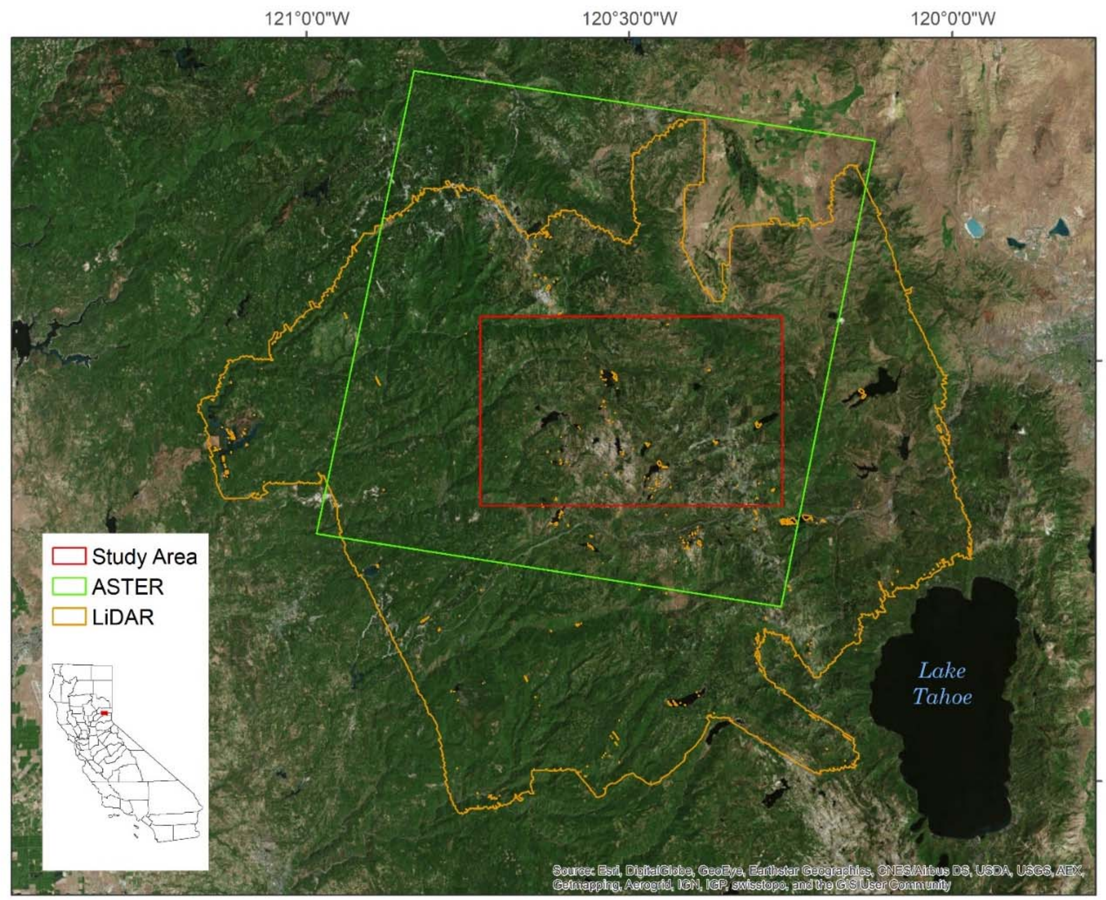

Fig. 1 Study area and the extent of ASTER and LiDAR data used. The LiDAR extend is approximately the same boundary as the Tahoe National Forest.

The vegetation of the study area follows the general pattern of Sierra Nevada plants. Plants with higher water requirements are found on the western slope of the range and the drier plants on the eastern side[1]. The western portion consists of ponderosa pine, Douglas-fir-mixed conifer forests which transition into red fir- and white fir-mixed conifer forest and lodgepole pine forest at higher elevations[1]. The eastern portion of the study area is characterized as Jeffrey pine forest [1].

2.2 Dataset

Multiple return LiDAR, provided by the Tahoe National Forest, was used to assess the physical structure of landforms. LiDAR data was collected in 2013 and 2014 with an average point density of 7-8 points per square meter and a point spacing of 0.29-0.48 m. The reported horizontal accuracy was between 2 and 72 cm and the vertical accuracy was 5-35 cm. LiDAR data were collected and processed with the National Center for Airborne Laser Mapping guidelines[25].

From LiDAR, the first return points and classified bare ground points were used to create a digital surface model (DSM) and a digital terrain model (DTM) respectively in ArcGIS® 10.4.1. The elevation difference between the DSM and DTM rasters was then used to create a canopy height model at 5 m resolution. From the DTM, slope, depressions, and flow accumulation were derived at 5 m resolution. Flow accumulation was calculated with the flow accumulation tool in ArcGIS. Five-meter resolution was found to depict tree crowns and stream channels. Topographic curvature was derived from the DTM at 20 m resolution. The 20 m resolution was found to best represented the general shape of the landforms at the meadow scale. In addition, a 1 m hillshade was derived from the bare ground LiDAR points. All data were processed to the extent of the study area.

A level 1A Advanced Spaceborne Thermal Emission Reflection Radiometer (ASTER) satellite image from July 24th, 2008 was acquired from the U.S. Department of the Interior U.S. Geological Survey (USGS) EarthExplorer data portal[26,27]. It was the most recent cloud-free ASTER image, taken during the growing season that covered the entire study area. ASTER was chosen because it had the highest resolution of freely available satellite imagery. The image was orthorectified in ERDAS Imagine® 2016 and atmospherically corrected with ATCOR 3® to produce the final image with bands of green, red, and near-infrared at 15 m resolution.

Google Earth® 7.1.8 was referenced for the ruleset creation and for the accuracy assessment. Specifically, Google Earth® historical imagery feature and 2.5D view were used as a visual aid during digitization. The historical imagery helped differentiate meadows from uplands. Due to the availability of shallow groundwater in meadows during the growing season, meadow vegetation stays green longer than upland vegetation. These seasonal greenness patterns were observed with the historical imagery from early summer and late summer. Through visual inspection of the historical images from winter and spring, water flow patterns and stream channels were located. Images from winter and spring were used because 1) plants were not leafed out and obscuring the streams, and 2) because water flow was higher making the flow patterns easier to decipher. In addition, because the canopy height raster was a single snapshot in time, the historical imagery was used to determine whether treeless areas were meadows or logged areas. Treeless areas potentially mistaken as meadows were inspected in the up to 24-year record of imagery to determine whether they were once forested. The Google Earth 2.5D view aided in assessing the topographic position of meadows for the hydrogeomorphic classification. Specifically, it was used to determine whether a meadow was located along a topographic drainage or at a toeslope.

The Tahoe National Forest meadow layer (TNF Meadows), provided by the Tahoe National Forest, was used for reference and accuracy assessment. It was updated from the Sierra Nevada Multi-Source Meadow Polygons Compilation (SNMPC) from the University of California, Davis[15]. SNMPC is a compilation of mapped meadows, equal to or greater than 0.4 ha, from various federal agencies, universities, non-profits, and science companies. In December 2016, the Tahoe National Forest locally updated the SNMPC. The update included the addition of unmapped meadows, removal of misidentified meadows, meadow boundary changes, and hydrogeomorphic classifications of meadows in the Tahoe National Forest. The TNF Meadows used ‘heads-up’ digitizing of 1 m National Agriculture Imagery Program (NAIP) imagery, topographic maps, and the National Hydrography Dataset for meadow detection and hydrogeomorphic classification[28]. The TNF Meadows were classified based on the hydrogeomorphic key in Weixelman (2016). The classes included: lacustrine fringe, riparian (low, middle, and high gradient), subsurface (low, middle, and high gradient), depressional (perennial and seasonal), discharge slope, and dry meadows. However, since the dataset was received, a simplified hydrogeomorphic key was released for future updates which included: lacustrine fringe, riparian, subsurface, depressional, discharge slope, and dry meadows[29].

2.3 Meadow Detection and Hydrogeomorphic Classification

Using OBIA with supervised decision tree classification, meadows were first *detected* and the detected meadows were then *classified* by hydrogeomorphic type (Fig. 2). The hydrogeomorphic class definitions (Table 1) were adapted from Weixelman (2017). Figure 3 shows representative examples of the hydrogeomorphic classes. The dry meadow class was not used because it was not discernably different from grasslands in the imagery and therefore, the classification accuracy could not be assessed with the presented methods.

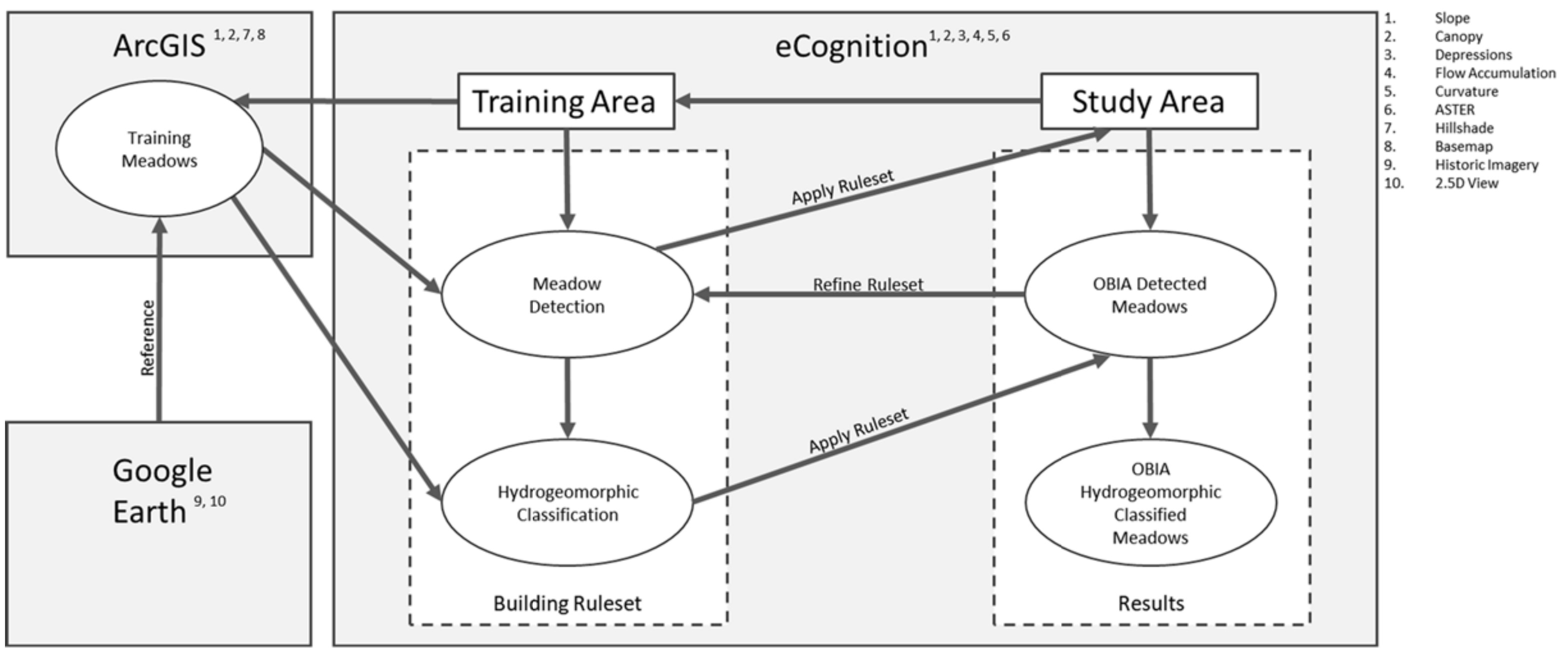

Fig. 2 Flow chart of OBIA detection and classification process including ruleset development.

Table 1 Hydrogeomorphic meadow classes used with descriptions

Hydrogeomorphic Classes	Dominant Water Source	Geomorphic Setting
Depressional	Precipitation, surface runoff, subsurface flow	Depressions less than 2m in depth
Discharge Slope	Groundwater upwelling, subsurface return flow, surface runoff	Hillslopes, toeslopes, slope breaks
Lacustrine Fringe	Subsurface seepage, overbank flow	Waterbodies greater than 2m in depth such as ponds or lakes
Riparian	Overbank flow from channel, subsurface flow	Stream with bed and bank stream morphology for majority of meadow
Subsurface	Subsurface flow, groundwater discharge, snowmelt surface runoff	Topographic flowline without bed and bank stream morphology for majority of meadow

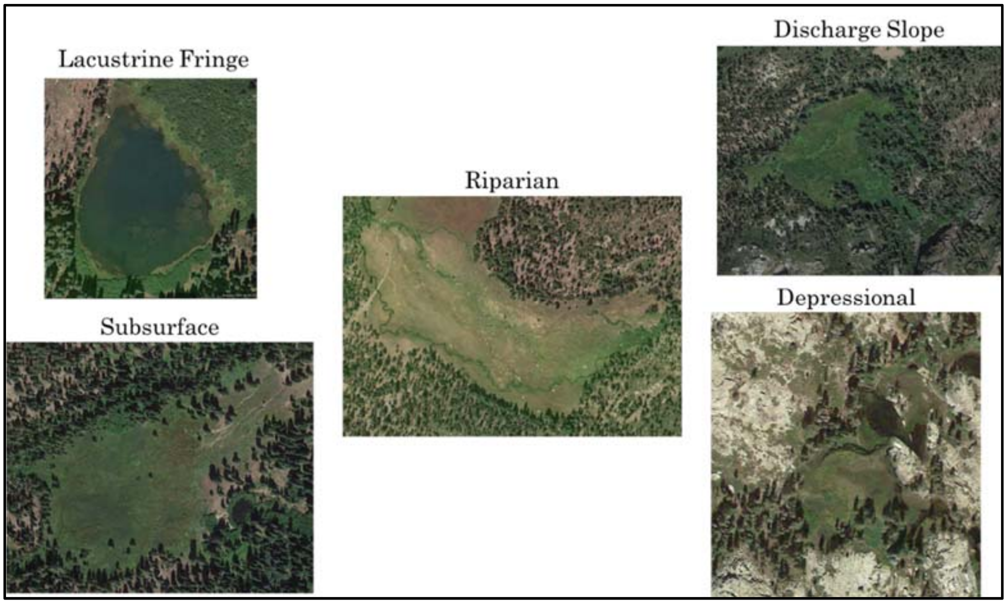

Fig. 3 Representative examples of the hydrogeomorphic classes.

In eCognition, the training meadows were overlaid on the primitive objects. Rules were created through trial and error to detect the objects overlain by the training meadows. Once, the training meadows were accurately detected, the ruleset was applied to the entire study area. Based on visual evaluation of the detection results, small modifications were made to the ruleset to improve the meadow detection.

Rules were then created that classified the detected meadow objects to match the corresponding hydrogeomorphic class of the training meadows. The ruleset was then applied to the entire study area. Based on visual evaluation of the classification results, modifications were made to the ruleset to improve the hydrogeomorphic classification.

2.3.1 Training meadows

In a representative 45 km^2 subset of the study area, all known meadows from visual inspection and the TNF meadows layer were digitized by hand and classified by hydrogeomorphic type to create training meadows. The subset was selected because all hydrogeomorphic types were present. The digitization was conducted in ArcGIS® 10.4.1, and used the hillshade to visualize stream channels, slope to determine flat areas conducive for meadows, canopy height to find treeless areas, and the ArcGIS high-resolution imagery basemap. In addition, Google Earth® historical imagery feature and 2.5D view were used as a visual reference for the digitization and hydrogeomorphic classification. The digitized training meadows were then used in eCognition to create the decision tree classification for meadow detection and classification.

2.3.2 Meadow detection

The first step in OBIA is to segment the data into primitive objects that best represents the phenomena being mapped[22]. In Trimble eCognition® Developer 9.1, a ruleset was created that segmented the dataset using the "multiresolution segmentation". For the segmentation, slope, canopy height, and the near-infrared band were used as the image layers. The input weights used were 0.1 for shape, 0.5 for compactness, and 5 for scale. Two identical segmentation were created. In the first segmentation, waterbodies were classified and the second segmentation non-meadow areas were classified and the waterbodies were superimposed. Then in the second segmentation, meadows were detected from the remaining non-classified objects. Waterbodies were classified in a separate segmentation because the classification ruleset included merging objects together which would have impacted the subsequent meadow detection and classifications.

In the first segmentation, waterbodies were classified. After testing several spectral indices calculated with the object features tools in eCognition, the Normalized Difference Water Index (NDWI) was used to aid in waterbodies classification[30]. NDWI is calculated from the difference of the NIR band and green band divided by the sum of the NIR and green band (equation 1).

$$NDWI = \frac{NIR - Green}{NIR + Green} \tag{1}$$

Primitive objects were classified as waterbodies based on the eCognition Brightness, mean slope, NDWI, and standard deviation of canopy height. Classified waterbody objects that shared a border were merged together. Upon visual inspection, the edges of waterbodies did not meet the classification criteria, and to classify them, waterbody objects were grown. This was achieved by classifying unclassified objects that shared a border with classified waterbody objects and then merged them together. Shaded areas were often misclassified as waterbodies. Due to the irregular shape of shadows, the misclassifications were eliminated if the objects were less than 1250 m^2 with an elliptic fit less than 0.5. The remaining objects were considered the final classified waterbody objects.

In the second segmentation copy, non-meadow areas were detected. Primitive objects outside of the digitized training meadows were classified as non-meadows using mean curvature, red near-infrared (NIR) ratio (equation 2), and mean slope[31].

$$Red\ NIR\ Ratio = \frac{Red}{NIR} \tag{2}$$

These objects represented ridges and narrow drainages classified by curvature, bare ground and upland vegetation classified by red near-infrared ratio, and areas with steep slopes classified by slope. The classified waterbody objects were then superimposed onto the second segmentation.

The remaining unclassified objects were then considered candidate meadows and were refined until the objects represented the location and shape of the training meadows. The objects were classified as Detected Meadow using maximum flow accumulation (highest flow accumulation pixel value within each object), mean slope, mean canopy, NDVI, and red NIR ratio[32]. NDVI is defined as:

$$NDVI = \frac{NIR-Red}{NIR+Red} \tag{3}$$

Maximum flow accumulation and mean slope were used to find areas of potentially shallow groundwater. Vegetated areas with short canopies were found with mean canopy height, mean NDVI, and mean red NIR ratio. To account for variation within meadows, objects that bordered the classified meadow objects were classified and then merged into one large meadow object. Then to eliminate misclassification, classified meadow objects less than 0.4 ha were unclassified. Again, neighboring objects were classified and merged if they shared a border with classified meadow objects and met additional slope and canopy criteria such as:

"Mean canopy less than 0.6 m and mean slope less than 3%."

Once the ruleset accurately classified the objects that represented the training meadows in the training area (Fig. 4), it was applied to the entire study area and refined based on the results. The largest meadows in the study area were detected as many small meadows. The ruleset was then modified by using the "relative border", "border to", and "merge" to better detect large meadows as one object. The ruleset was again applied to the entire study area to produce the final OBIA detected meadow results.

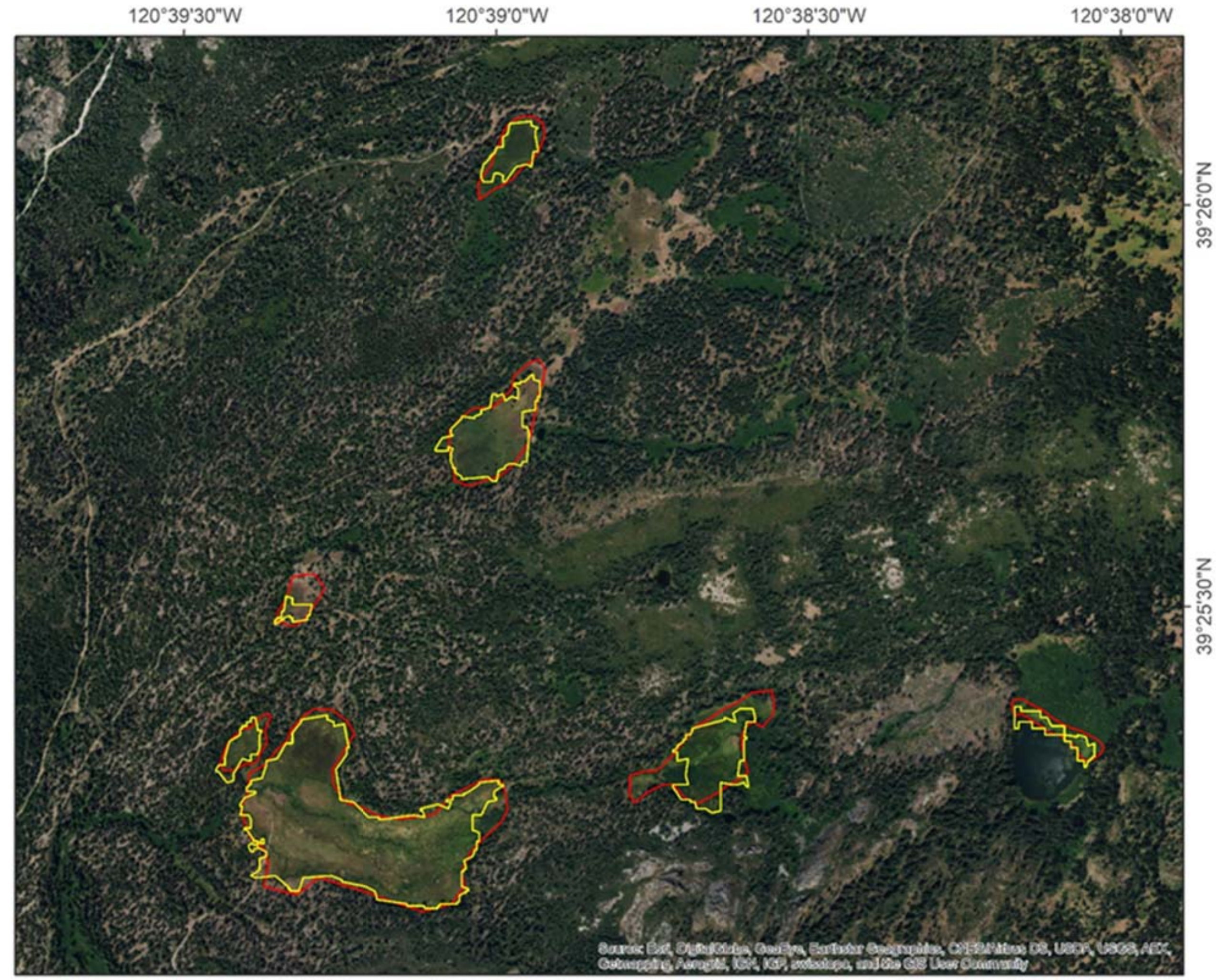

Fig. 4 Training meadows (red) and OBIA detected meadows (yellow) in a subset of the training area used for ruleset creation.

2.3.3 OBIA meadow hydrogeomorphic classification

The OBIA hydrogeomorphic classification ruleset was developed using the training meadows in the subset area and applied to the OBIA detected meadows. OBIA detected meadows were classified in order: lacustrine fringe, depressional, riparian, subsurface, and discharge slope. Figure 5 shows the logical process of OBIA hydrogeomorphic classification.

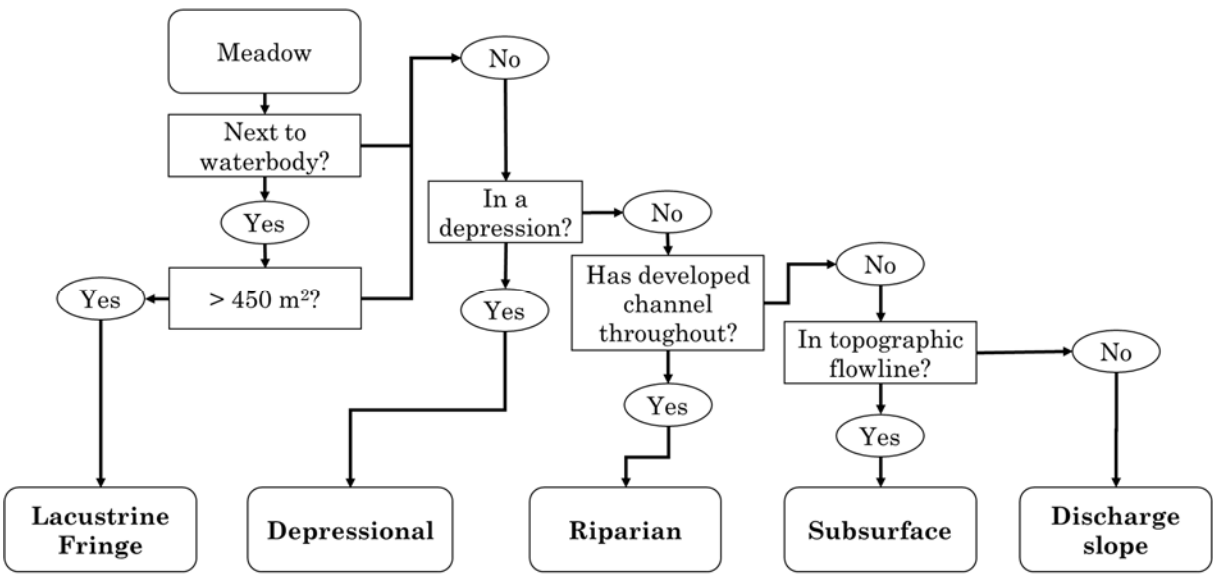

Fig. 5 The logical flowchart from which the meadow hydrogeomorphic classification ruleset was developed.

OBIA detected meadows adjacent classified waterbodies were classified as lacustrine fringe with the "border to" function. Next, depressional meadows were classified using the mean depressions. Depressional meadows were found to be smaller than most other meadows so a size limit of 1.25 ha was used. Riparian, subsurface, and discharge slope were all classified using maximum flow accumulation. Maximum flow accumulation areas greater than 25 km^2 were found to have fully developed stream channels throughout the meadow and were used to classify riparian meadows. Maximum flow accumulation area of greater than 0.14 km^2 and equal to 25 km^2 were associated with meadows that did not have stream channels with bed and bank morphology throughout and were used to classify subsurface meadows. Finally, discharge slope meadows were found to have a maximum flow accumulation area of less than 0.14 km^2, and the remaining detected meadows were classified as discharge slope. Once hydrogeomorphic classification of the OBIA detected meadows was in agreement with the corresponding training meadows, it was applied to the remaining OBIA detected meadows in the entire study area.

2.4 Accuracy Assessment

Accuracies of the OBIA detected meadows and OBIA hydrogeomorphic classified meadows were determined using two assessment methods, following Congalton and Green (2009). The first compared the OBIA detected meadows to manually detected meadows and to the TNF Meadows. The second compared the OBIA classified meadows to manually classified meadows and TNF Meadows. Extensive ground truthing was not possible due to the remote location of many meadows.

The accuracy of the OBIA detected meadows compared to manually detected and TNF Meadows was assessed using randomly stratified points. This method was selected because the detected meadows only occupied a small portion of the study area. The training area and the large meadows used to refine the OBIA detection and classification ruleset were excluded from the accuracy assessment. In ArcGIS, 200 of the OBIA detected meadows were randomly selected and received a random point designated “meadow.” Three-hundred random “other” points were placed outside of meadows in the study area. Both “meadow” and “other” random point sets were merged into a single dataset. For the manually detected meadows, each point was manually assigned as “meadow” or “other” using the methods used for the training meadows and accuracies were calculated accordingly[33]. For the TNF Meadows, the point was classified as “meadow” if it was located within a meadow polygon and the accuracies were calculated.

For the hydrogeomorphic classification accuracy assessment, the accuracy of the OBIA classified compared to manually classified meadows was assessed by inspecting every meadow that was accurately detected per the manually detected meadows. With the OBIA classification results hidden, the accurately detected OBIA meadows were manually classified using the same classification methods as the training meadows, and the accuracies were calculated accordingly[33]. For the TNF Meadows, each meadow point that was accurately detected, according to the OBIA detected and the TNF meadows, was used. Each point was given the hydrogeomorphic class of the corresponding TNF Meadows polygon and compared to the OBIA classified meadows. The accuracies were then calculated. The distribution of all the hydrogeomorphic classes were compared for the OBIA classified, manually classified, and TNF Meadows.

3 Results

3.1 Meadow Detection

The OBIA detected meadows produced a 98% overall accuracy when compared to the Manually Detected meadows (Table 2). Of the 200 points placed within the OBIA detected meadows, 195 were confirmed to be meadows in the manual detection. The manual detection found 3 of the 300 points placed outside of the OBIA detected meadows to be meadows. User's accuracy of meadows was using was 98%, and producer's accuracy was 98%.

The overall accuracy of detection was lower when comparing OBIA detected meadows to TNF Meadows at 91% (Table 3). Of the 200 OBIA meadows points, 158 were in agreement with the TNF Meadows. User's accuracy of meadows was 79%, and producer's accuracy was 98%.

Table 2 Meadow detection accuracy assessment comparing OBIA detected and manually detected meadows.

		Manually Detected			User's Accuracy
		Meadow	Other	*Total*	
OBIA Detected	Meadow	195	5	200	98%
	Other	3	297	300	99%
	Total	198	302	500	
Producer's Accuracy		98%	98%		Overall Accuracy 98%

Table 3 Meadow detection accuracy assessment comparing OBIA detected and TNF meadows.

		TNF Meadows			User's Accuracy
		Meadow	Other	*Total*	
OBIA Detected	Meadow	158	42	200	79%
	Other	3	297	300	99%
	Total	161	339	500	
Producer's Accuracy		98%	88%		Overall Accuracy 91%

3.2 Hydrogeomorphic Classification

Figure 6 shows a section of the final OBIA detection and classification. For the hydrogeomorphic classification accuracy, the OBIA classified meadows compared to the Manually Classified meadows had an overall accuracy of 82% (Table 4). The user's accuracy varied with the discharge slope class the lowest at 64% accuracy and lacustrine fringe class the highest at 93% accuracy. Producer's accuracy also varied, with the depressional class at only 38% and the lacustrine fringe at 93%.

The overall accuracy of hydrogeomorphic classification was lower when comparing OBIA classified meadows to TNF Meadows at 35% (Table 5). The user's accuracy ranged broadly, with the depressional class at 0% and riparian class at 100%. The producer's accuracy also ranged broadly, with the depressional class 0% and the lacustrine fringe class at 86%.

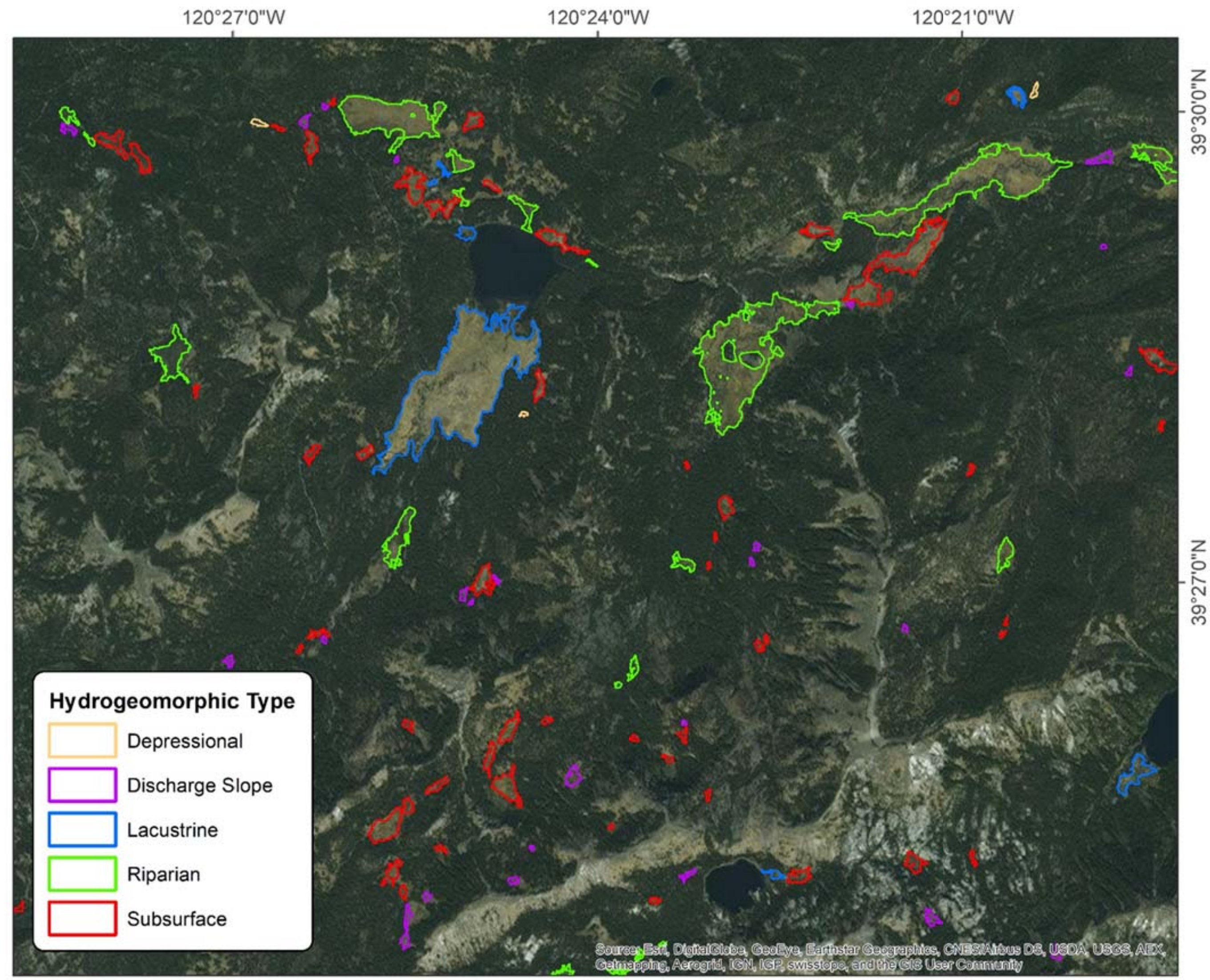

Fig. 6 A subset of the OBIA meadow detection and classification results.

Table 4 Meadow hydrogeomorphic classification accuracy assessment comparing OBIA classified and manually classified meadows.

		Manually Classified						User's Accuracy
		Depressional	Discharge Slope	Lacustrine Fringe	Riparian	Subsurface	*Total*	%
OBIA Classification	Depressional	3	0	0	0	1	4	75%
	Discharge Slope	2	23	0	0	11	36	64%
	Lacustrine Fringe	1	0	14	0	0	15	93%
	Riparian	0	0	0	44	7	51	86%
	Subsurface	2	5	1	6	75	89	84%
	Total	8	28	15	50	94	195	
Producer's Accuracy	%	38%	82%	93%	88%	80%		
						Overall Accuracy	82%	

Table 5 Meadow hydrogeomorphic classification accuracy assessment comparing OBIA classified and TNF Meadows.

		TNF Meadows						User's Accuracy
		Depressional	Discharge Slope	Lacustrine Fringe	Riparian	Subsurface	*Total*	%
OBIA Classified	Depressional	0	0	0	1	0	1	0%
	Discharge Slope	0	4	0	18	4	26	15%
	Lacustrine Fringe	1	1	6	3	0	11	55%
	Riparian	0	0	0	43	0	43	100%
	Subsurface	3	1	1	69	3	77	4%
	Total	4	6	7	134	7	158	
Producer's Accuracy	%	0%	67%	86%	32%	43%		
						Overall Accuracy	35%	

4 Discussion

OBIA detected meadows corresponded well with both the Manually Detected meadows (98% overall accuracy) and the TNF Meadows (91% overall accuracy). The detection accuracy assessment found 37 meadows in agreement with both the OBIA detection and manual detection and not with the TNF meadows. The TNF meadows had 10 of the meadows but they were misdetected because the accuracy assessment point fell outside of the TNF meadows delineation. However, 27 of the meadows in agreement with both the OBIA detection and manual detection were completely missed by the TNF meadows. These meadows were found throughout the study area and had a combined area of 21.18 ha with a median size of 0.67 ha.

Most of the OBIA detected meadows that were not meadows when compared to Manual or TNF Meadows were associated with waterbodies that appeared to be eutrophic or had aquatic vegetation growing on the surface (Fig. 7a). The aquatic vegetation produced a NDVI value that met the threshold for meadow vegetation which ultimately caused the misdetection. Some OBIA detected meadows were found to be logged areas (Fig. 7b & c). These areas were logged between when the ASTER image was taken and the LiDAR was collected. In the ASTER image, the objects were green and forested, but in the LiDAR, the objects were treeless. This caused misdetection because the objects met the Red NIR Ratio, NDVI, and canopy rules for meadows detection.

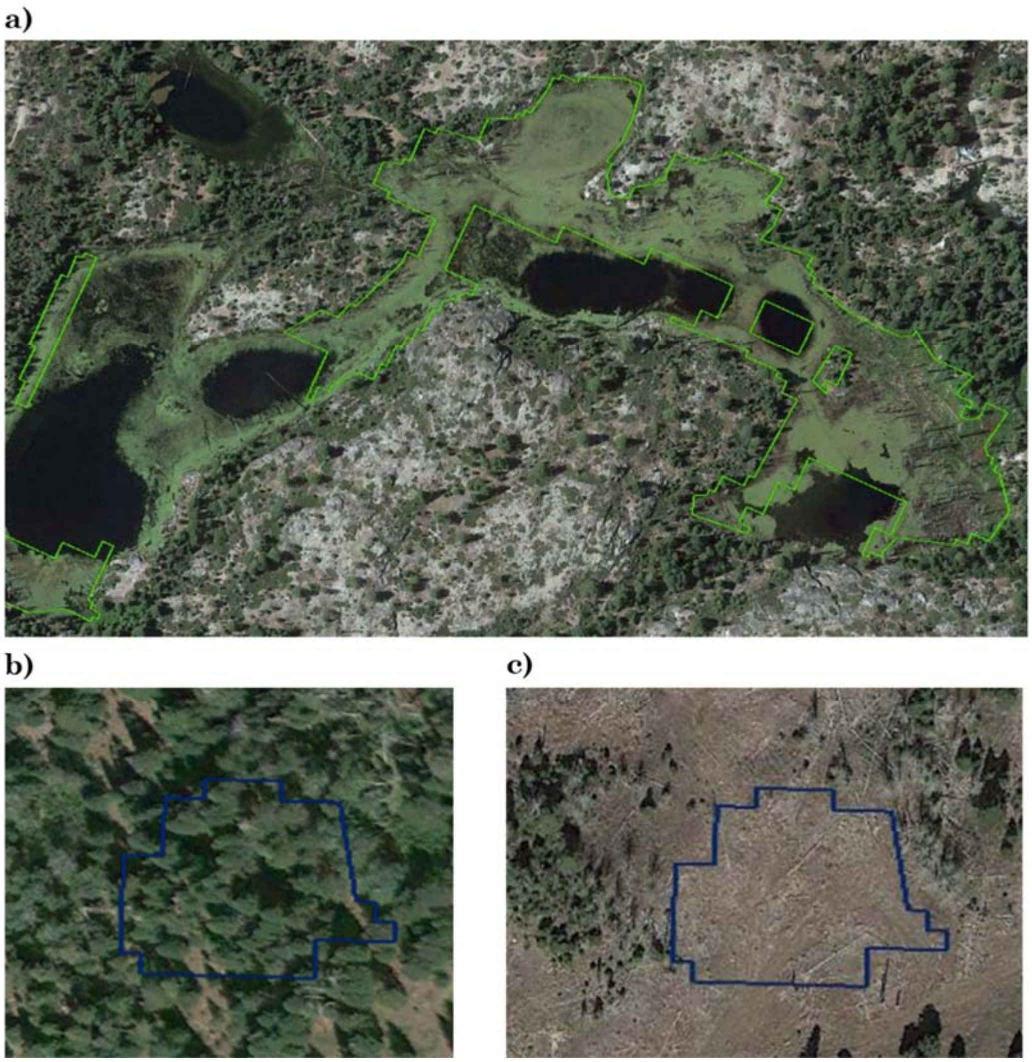

Fig. 7 OBIA detected meadows that were not meadows. a) Eutrophic waterbody detected as a meadow. b) Google Earth image from 8/28/2012 of an area detected as meadow before being logged. c) Google Earth image from 4/29/2014 of the same detection after being logged.

Only one meadow was not detected by the OBIA method but was identified manually and by TNF Meadows. This meadow was not detected because it did not meet the curvature thresholds in the ruleset. At the location of the meadow the curvature raster was too convex. However, upon visual inspection in Google Earth, the meadow does not appear to be convex. This is most likely a blunder in the LiDAR data being propagated through the derived curvature raster. The curvature raster was derived from the DTM which was based on the bare earth returns of the LiDAR. If a non-bare earth point was classified as a bare earth point than the interpolated DTM would have a higher elevation at the location than it should and thus, lead to the convex result.

Two meadows were not detected by the OBIA detection or by TNF meadows but were manually detected. One was missed because a large proportion of the meadow area was made up of a stream with exposed gravel banks which lowered the NDVI, used to determine the vegetation presence, below the set threshold. The other meadow was not detected because the accuracy assessment point was located just outside of the meadow boundary according to the OBIA detection but was found to be within the defined meadow boundary in the visual detection. Finally, two meadows were not detected by the OBIA detected or manually detected meadows but were detected by TNF meadows. For both, the accuracy assessment points were in forested areas, near a meadow, that did not meet the low canopy threshold of the stated meadow definition.

Similar to the meadow detection results, the OBIA hydrogeomorphic classification when referenced to manual classification resulted in higher accuracy (82%) than TNF Meadows (35%). OBIA meadow classification performed very well for some classes. When compared to the Manually Classified Meadows, lacustrine fringe class had a user's and producer's accuracy of 93%. It also, performed well for riparian meadows with a user's accuracy of 82% and a producer's accuracy of 88%. While the other results are lower, steps could be incorporated in future research to improve the numbers.

The lower hydrogeomorphic accuracy for OBIA classification compared to TNF meadows may be due to slight differences in interpreting the hydrogeomorphic class definitions. Comparing the hydrogeomorphic class distributions of the three classification methods (Fig. 8), the OBIA classification and Manual classification had a similar distribution of classes with subsurface as the most common hydrogeomorphic class. The TNF Meadows had a different distribution of classes with riparian being the most common class. Upon visual inspection of the TNF Meadows in Google Earth, meadows with a runoff channel from an adjacent hill slope were often classified as riparian. However, based on the hydrogeomorphic definitions from Weixelman (2017), riparian meadows have developed bed and bank morphology, and these meadows did not. These same meadows were often classified as discharge slope by the OBIA and Manual classification. This could be evidence that the TNF Meadows and OBIA classification had differing interpretations of the hydrogeomorphic class definitions.

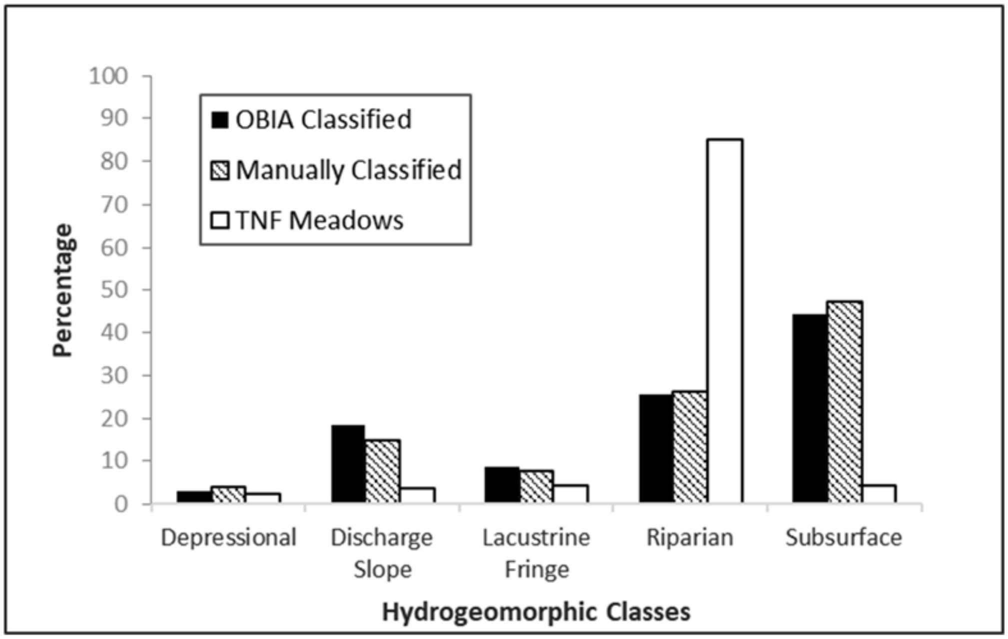

Fig. 8 The percentage of each hydrogeomorphic class by classification method: OBIA classified (black), manually classified (stripes), and TNF Meadows (white). TNF Meadows had a much higher percentage of riparian meadows than OBIA classified and the manually classified meadows. See text for explanation.

There were several reasons for misclassification of the OBIA Hydrogeomorphic Classification compared to Manual Classification. Depressional meadows (75% user's and 38% producer's) classification relied on the initial depression raster derived from the LiDAR. Any blunders, such as shrubs not being filtered out in the initial LiDAR processing, could impact the depths of the depressions and in turn cause confusion with the class thresholds. Discharge slope and subsurface meadows and subsurface and riparian meadows were often confused for one another.

5 Conclusion

This study demonstrated a remote sensing method using OBIA for semi-automated detection and classification of meadows. Meadows in the study area within the Tahoe National Forest were detected using LiDAR and multispectral imagery and classified by hydrogeomorphic type using physical characteristics derived from LiDAR. The presented methods for meadow detection and hydrogeomorphic classification could be a valuable tool for land managers.

This study is unique in its focus on meadows, however, it is comparable to wetland classification studies. Halabisky et al. (2011) used OBIA with hierarchical decision tree to classify wetlands in Washington. Like this study, it used a customized rule set which allows for site specific application of expert knowledge. Rampi et al. (2014) used OBIA with LiDAR and high-resolution imagery to classify wetlands from surrounding land covers. They found that the inclusion of high-resolution LiDAR and derivatives improved the differentiation of wetlands from the other land covers compared to using spectral data alone. Similar results were presented here.

The use of LiDAR derivatives aided in the detection and classification of meadows, and added information that could not have been derived from spectral data alone. The LiDAR derivatives, which were used to analyze meadow morphology, was just as important as the spectral reflectance of the satellite imagery for detection. For the hydrogeomorphic classification, the LiDAR derivatives were exclusively used to differentiate between the various hydrogeomorphic meadow types. Overall, use of LiDAR was critical to achieve that detection and classification results.

Further research could improve meadow detection and hydrogeomorphic classification. Meadow detection, could be improved by using multitemporal imagery. Multitemporal imagery could be used to detected logged areas that would otherwise be detected as meadows (Fig. 7). Hydrogeomorphic classification could be improved by incorporating climate data. Geographic climate models, such as PRISM, could add nuance to the watershed areas thresholds values.

Meadows play important ecological roles in the mountainous landscapes. Knowing where and how many meadows exist is critical for researcher and land managers. Remote sensing can be a powerful tool to aid in the detection and classification of meadows throughout the Sierra Nevada and mountainous regions around the world.

References

1. J. A. Fites-Kaufman, et al., "Montane and Subalpine Vegetation of the Sierra Nevada and Cascade Ranges," in, *Terrestrial Vegetation of California*, (ed. Barbour, M.), 456–501 (University of California Press, 2007).
2. C. T. Hammersmark, M. C. Rains, & J. F. Mount, "Quantifying the hydrological effects of stream restoration in a montane meadow, northern California, USA," *River Res. Appl.*, (24), 735–753 (2008).
3. R. Kattelmann, & M. Embury, "Riparian areas and wetlands," *Sierra Nevada Ecosyst. Proj.*, (III), 34–68 (1996).
4. R. D. Ratliff, *A Meadow Site Classification for the Sierra Nevada , California General Technical Report PSW*, (1982).
5. J. B. Norton, et al., "Soil Carbon and Nitrogen Storage in Upper Montane Riparian Meadows," *Ecosystems*, **8**(14), 1217–1231 (2011).
6. R. H. Barrett, et al., *California wildlife and their habitats: western Sierra Nevada Gen. Tech. Rep. PSW-GTR-37*, (1980).
7. R. A. Knapp, "Effects of nonnative fish and habitat characteristics on lentic herpetofauna in Yosemite National Park, USA," *Biol. Conserv.*, **2**(121), 265–279 (2005).
8. W. D. Spencer, R. H. Barrett, & W. J. Zielinski, "Marten Habitat Preferences In The Northern Sierra Nevada," *J. Wildl. Manage.*, **4**(47), 1181–1186 (1983).
9. D. A. Weixelman, et al., *A Field Key to Meadow Hydrogeomorphic Types for the*

Sierra Nevada and Southern Cascade Ranges in California (2011).

10. R. F. Holland, *Preliminary description of the terrestrial natural communities of california* (1986).

11. B. H. Allen, "Forest and meadow ecosystems in California," *Rangelands*, **3**(9), 125–128 (1987).

12. N. B. Benedict, & J. Major, "A physiographic classification of subalpine meadows of the Sierra Nevada, California.," *Madrono*, **1**(29), 1–12 (1982).

13. R. D. Ratliff, *Meadows in the Sierra Nevada of California: state of knowledge General Technical Report PSW-84*, (1985).

14. M. M. Brinson, *A Hydrogeomorphic Classification for Wetlands, Technical Report WRP-DE-4* (1993).

15. A. Fryjoff-Hung, & J. H. Viers, *Sierra Nevada Multi-Source Meadow Polygons Compilation (v 1.0)* **December** (2012).

16. J. H. Viers, et al., *Montane Meadows in the Sierra Nevada: Changing Hydroclimatic Conditions and Concepts for Vulnerability Assessment Center for Watershed Sciences Technical Report (CWS-2013-01)*, (2013).

17. A. M. B. May, J. E. Pinder III, & G. C. Kroh, "A comparison of Landsat Thematic Mapper and SPOT multi-spectral imagery for the classification of shrub and meadow vegetation in northern California, USA," *Int. J. Remote Sens.*, **18**(18), 3719–3728 (1997).

18. S. L. Ozesmi, & M. E. Bauer, "Satellite remote sensing of wetlands," *Wetl. Ecol.*

Manag., (10), 381–402 (2002).

19. Z.-T. Ouyang, et al., "A Comparison of Pixel-Based and Object-Oriented Approaches to VHR Imagery for Mapping Saltmarsh Plants," *Ecol. Inform.*, **2**(6), 136–146 (2011).

20. O. Usmerjena, A. Podatkov, & D. Zaznavanja, "Object-based image analysis of remote sensing," *Geod. Vestn.*, **4**(55), 665–688 (2011).

21. U. C. Benz, et al., "Multi-resolution, object-oriented fuzzy analysis of remote sensing data for GIS-ready information," *J. Photogramm. Remote Sens.*, (58), 239–258 (2004).

22. K. B. Moffett, & S. M. Gorelick, "Distinguishing wetland vegetation and channel features with object-based image segmentation," *Int. J. Remote Sens.*, **4**(34), 1332–1354 (2013).

23. "BOWMAN DAM, CALIFORNIA: Period of Record General Climate Summary - Precipitation," *Western Regional Climate Center*, (2012). Available at: http://www.wrcc.dri.edu/cgi-bin/cliGCStP.pl?ca1018. (Accessed: 2nd May 2017)

24. "SAGEHEN CREEK, CALIFORNIA: Period of Record General Climate Summary - Precipitation," *Western Regional Climate Center*, (2012). Available at: http://www.wrcc.dri.edu/cgi-bin/cliGCStP.pl?ca7641. (Accessed: 2nd May 2017)

25. *NCALM Data Collection & Processing Summary* **November** (2016).

26. USGS Earth Resources Observation and Science (EROS), "NASA LP DAAC, ASTER Level 1A," (2016).

27. U.S. Department of the Interior U.S. Geological Survey, "EarthExplorer," (2016). Available at: https://earthexplorer.usgs.gov/. (Accessed: 7th December 2016)

28. D. A. Weixelman, "Tahoe National Forest Meadow Polygon Update," (2016).

29. D. A. Weixelman, "USFS Mapping meadow hydro-geomorphic (HGM) types (Unpublished)," (2017).

30. S. K. McFeeters, "The use of the Normalized Difference Water Index (NDWI) in the delineation of open water features," *Int. J. Remote Sens.*, **7**(17), 1425–1432 (1996).

31. M. Halabisky, L. M. Moskal, & S. A. Hall, "Object-based Classification of Semi-arid Wetlands," *J. Appl. Remote Sens.*, **1**(5), 1–13 (2011).

32. L. P. Rampi, J. F. Knight, & K. C. Pelletier, "Wetland Mapping in the Upper Midwest United States : An Object-Based Approach Integrating Lidar and Imagery Data," *Photogramm. Eng. Remote Sens.*, **5**(80), 439–449 (2014).

33. R. G. Congalton, & K. Green, *Assessing the Accuracy of Remotely Sensed Data: Principles and Practices* (Taylor & Francis Group, 2009).